Laminar Velocity Profiles in Developing Flows using a Laser Doppler Technique

NEIL S. BERMAN and VALERIO A. SANTOS
Arizona State University, Tempe, Arizona

A laser doppler flowmeter is used to obtain velocity profiles in circular glass tubes downstream from a plug composed of brass screens. The apparatus for measuring point velocities of particles suspended in a fluid is described. Measurements were made very close to the plug at Reynolds numbers of 16.5, 47, and 274, and the flow development followed down the tube. The results show that the entrance flow development is dependent on the inlet profile shape and the Reynolds number for Reynolds numbers below 300.

The flow development at Reynolds numbers less than 300 was considerably slower than that predicted by the boundary-layer solution of the equations of motion starting with a flat profile.

Experimental data on velocity profiles in the entrance region of circular conduits are available only down to a Reynolds Number of 450. At lower Reynolds Numbers point velocities have been difficult to measure.

A new method for measuring local flow velocities in fluids is an optical doppler technique. When monochromatic light is scattered from moving particles in a fluid stream, the frequency of the scattered light differs from that of the incident light. This frequency shift can be measured by combining the scattered and unscattered light at a photomultiplier when a suitable light source, such as a gas laser, is used. The bandwidth of the laser radiation is small enough so that doppler shifts corresponding to extremely small velocities can be measured. Also the light can be focused to a small spot making possible measurements of the velocity vectors in a small volume of fluid without disturbing the flow. In this work the laser doppler method is used to determine velocity profiles following a plug made of brass screens.

By using water with a small amount of polystyrene spheres added, velocity profiles were obtained at distances downstream of the plug starting at 1.5 mm. and at Reynolds Numbers of 16.5, 47, and 274 in a 1 cm. diam. glass tube. Other measurements of centerline development only were obtained for Reynolds Numbers of 109 and 460 and for different pipe sizes and screen mesh.

THE LASER DOPPLER TECHNIQUE

Review of Previous Work

The first measurement of velocity profiles in a fluid by using an optical doppler technique was by Yeh and Cummins (*1*). Cummins, Knable, and Yeh had previously investigated the diffusion broadening of laser light scattered from polystyrene spheres (*2*). These spheres were used as scattering media in the flow experiments at average velocities from .008 cm./sec. to .025 cm./sec. One part of monodispersed polystyrene spheres of diameter .557 μ was placed in 30,000 parts of water by volume. At room temperature the diffusion velocities were negligible.

Shortly after Yeh and Cummins demonstrated the basic principle, Forman, George, and Lewis (*3*) measured velocity profiles from 1 to 100 cm./sec. in a gas stream. They used optical focusing of both local oscillator and scattered beams and focused the combined signal on the photomultiplier. A frequency meter was used to monitor the signal. Foreman, et al., (*4*) (*5*) have refined their apparatus so that no particle scatterers are necessary in liquids; they extended the range of liquid velocity measurements well into the turbulent range and for gas velocity measurement to speeds greater than the velocity of sound.

Welch and Toome (*6*) used electronic processing to measure the spread of turbulent velocities at various points in a pipe. A Fabry-Perot scanning plate interferometer was used by James, Seifert and Babcock (*7*) to detect the doppler signal.

More recently Goldstein and Kreid (*8*) and Goldstein and Hagen (*9*) have used the laser doppler method to measure the flow of water in square ducts and in turbulent flow.

Doppler Effect

The doppler effect is named after Christian Doppler who gave an explanation in 1842 for the higher frequency of a train whistle as it approached an observer and the lower frequency as the train went away from the observer. An observer on a particle moving away from a fixed source of light would see light with a lower frequency than the source, and the scattered light would appear to have a different frequency from that detected by a stationary observer. The geometry of this situation is shown in Figure 1 where $\mathbf{k}_i$ and $\mathbf{k}_s^*$ are unit direction vectors of the incident and scattered light waves respectively, and $\mathbf{v}$ is the velocity of the particle.

The velocity of the wave, relative to the observer, can be obtained from the observed frequency multiplied by the wave length of the wave or from the difference between the velocity of light and the velocity of the observer in the wave direction. For an observer on the particle

$$\lambda_i \nu_p = C - \mathbf{k}_i \cdot \mathbf{v} \tag{1}$$

for the incident wave, and

$$\lambda_s \nu_p = C - \mathbf{k}_s \cdot \mathbf{v} \tag{2}$$

for the scattered wave.

Here, C is the velocity of light, ν_p, the frequency observed by the particle and λ_i and λ_s the wave lengths of the incident and scattered light respectively.

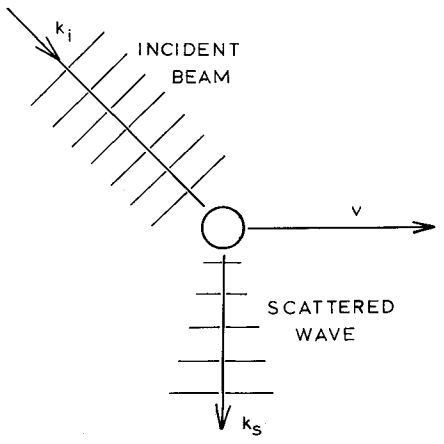

Fig. 1. Scattering geometry.

Taking the ratio of the two equations

$$\frac{\lambda_i}{\lambda_s} = \frac{C - \mathbf{v} \cdot \mathbf{k}_i}{C - \mathbf{v} \cdot \mathbf{k}_s} \tag{3}$$

By using $C = \lambda\nu$ and solving for $\Delta\nu = \nu_s - \nu_i$ we obtain

$$\Delta\nu = \frac{\frac{\nu_i \mathbf{v}}{C} \cdot (\mathbf{k}_s - \mathbf{k}_i)}{1 - \frac{\mathbf{v} \cdot \mathbf{k}_s}{C}} \tag{4}$$

When $\frac{\mathbf{v} \cdot \mathbf{k}_s}{C} << 1$,

$$\Delta\nu = \frac{\nu_i}{C} \mathbf{v} \cdot (\mathbf{k}_s - \mathbf{k}_i) \tag{5}$$

In terms of the vacuum wavelength, λ_o, and the index of refraction, n, we obtain

$$\Delta\nu = \frac{n}{\lambda_o} \mathbf{v} \cdot (\mathbf{k}_s - \mathbf{k}_i) \tag{6}$$

Optical Heterodyning

When the incident or local oscillator wave and the scattered wave are combined at the photomultiplier under proper conditions, a beat signal will be produced similar to the heterodyning of radio waves. If both signals are plane waves and the phase variation between signals is to be less than one wavelength across the aperture, then the wave fronts must be nearly parallel. Fringes will appear which will mask part or all of the beat signal when this phase variation is greater than one wavelength.

Other arrangements at the photomultiplier are discussed by Siegman (*10*). Optical elements placed in front of the photocathode will change the effective aperture and field of view subject to the constraint $A_R\Omega_R \sim \lambda^2$ where A_R is the area of the aperture and Ω_R the solid angle. With the sacrifice of some signal strength the angle may be made larger with a coresponding reduction in aperture size.

EXPERIMENTAL APPARATUS

The laser doppler flowmeter consists of the lasser and associated optical equipment so that the doppler shift can be measured. In this work the beam from a helium-neon laser was split into two beams. One was focused at a point in the moving fluid. Scattered light was then collected by a lens at an angle of approximately 10 deg. This scattered light and the second beam from the laser combined at the photo cathode of a photomultiplier tube. The beat signal was analyzed by a spectrum analyzer with the maximum signal taken as proportional to the velocity at a point in the moving fluid.

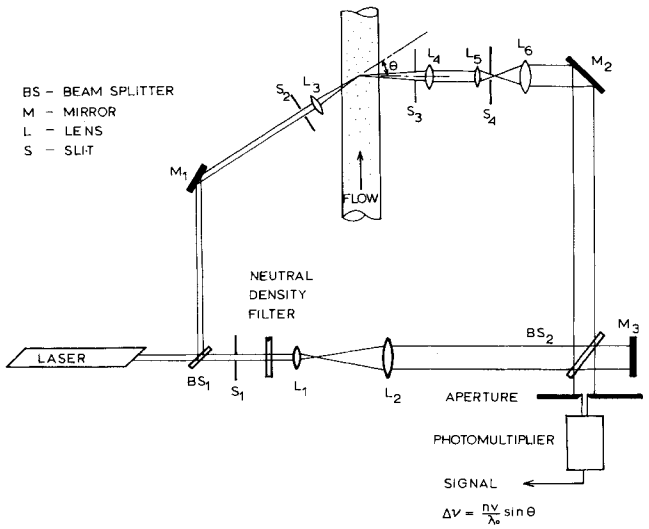

Fig. 2. Schematic diagram of a laser doppler flowmeter.

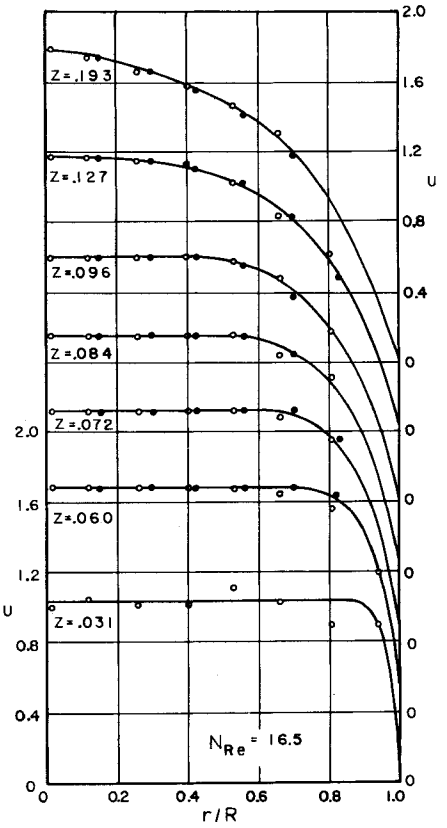

Fig. 3. Flow development in 1 cm. tube at $N_{Re} = 16.5$

A diagram of the apparatus is shown in Figure 2. A Perkin-Elmer Model 5220 laser with 5201 power supply was used as the light source. As an aid to optical alignment, the laser was modulated with a Hewlett 202B audio oscillator. No modulation was used during velocity measurements. The photomultiplier was an RCA 7265.

The local oscillator beam was expanded to approximately 1 in. in diameter by lenses L_1 and L_2 so that the beam was parallel at the photomultiplier. Neutral density filters were used to equalize the intensity of local oscillator and scattered beams. The reflected light back through mirror M_2 was used to make sure the scattered and unscattered beams in the flow tube were in the same plane. The scattered light was collected by lens L_4. Optical heterodyning was achieved by adjusting mirror M_3 so that the two beams were coaxial.

When $\mathbf{v}$, $\mathbf{k}_s$, and $\mathbf{k}_i$ are all in horizontal plane in the configuration shown in Figure 2,

$$\Delta\nu = \frac{nv}{\lambda_o} \sin\theta \tag{7}$$

The scattered light is shown perpendicular to the tube, however, the equation is the same if the incident beam is perpendicular to the tube. After the tests from both arrangements, it was found that measurements much closer to the tube wall could be made by using the pictured configuration.

Equation (7) indicates that the angle θ can be determined from the geometry, however, the size and position of the aperture the location of lenses L_4, L_5, L_6, and the relationship of the local oscillator and scattered beams all determined the point of measurement in the flow tube when the scattering volume was selected at the photomultiplier tube. If the tube is circular the sides of the tube also act as a lens further complicating the matter. The aperture in front of the photomultiplier tube was adjusted so that the light from an area only 2 mm. in diameter could pass through. Since the beam at this point had been expanded to a diameter of 1 in., the precise point in the tube corresponding to the source of the scattered light was difficult to determine by geometric measurements. Under these conditions, the scattering volume was at most 10^{-7} cc.

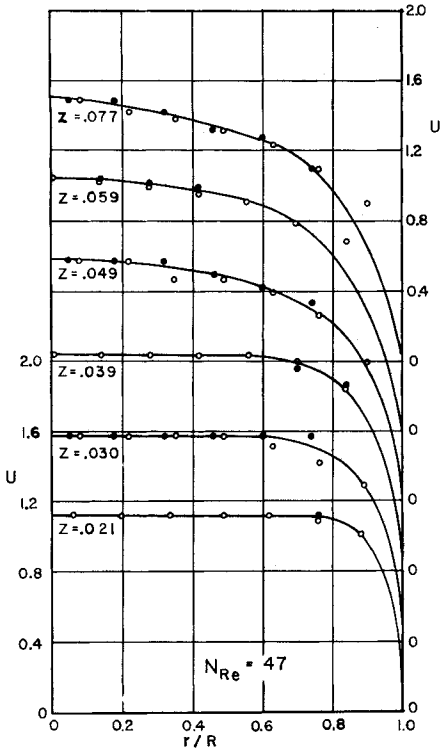

Fig. 4. Flow development in 1 cm. tube at $N_{Re} = 47$.

The apparatus was calibrated with a ground glass wheel mounted on a constant speed motor. This calibration had to be run in air which has a different index of refraction from the water used in flow experiments. It was possible to obtain accurate results by using the lens arrangement for optimum signal during the fluid flow runs when the calibration runs were made even though the point of intersection of the two beams was not at the focus of lens L_4. The calibration was checked by comparing the volume rate of flow by integrating the velocity profile with that obtained by collecting the flow.

The signal from the photomultiplier was sent directly to a Singer Metrics Panoramic Model SB-15a Spectrum Analyzer. Quantitative measurements were made by recording the spectrum analyzer display either photographically or with an x-y recorder. The peak signal was taken to be the average velocity at the measured point.

The flow tube was rigidly mounted on a milling table which could be moved in any direction. Scale divisions on the milling table feed handles were graduated in thousandths of an inch. The flow tube could then be moved either axially or radially to measure velocity profiles. At low velocities any transient signal introduced by movement of the mill table was found to die out within a second or two. This was checked by recording each pass of the spectrum analyzer.

A constant head tank was used to obtain steady flow conditions through a 4 ft. section of 1 cm. diam. standard wall glass pipe for most of the measurements. The flow rate was determined by collecting and weighing the effluent. By following the example of Atkinson, et al. (*11*), a set of screens was used to create an entrance flat profile. Several tests were run by using 40 mesh screens mounted in different ways. Twenty-five screens were set in place with each screen weave at 45 deg. to those adjacent. When a torpedo was used upstream to the screens, no effect was noted at low Reynolds numbers. At higher Reynolds numbers vortices were introduced when the torpedo was placed too close to the screens. Therefore, for the measurements in this work only the screens were used with no other obstruction in the tube. The screens were punched from a sheet using a hardened steel punch machined to the diameter of the tube. Measurements using this arrangement could be repeated with excellent precision on different tubes.

Extensive tests were run when the last screen and every fourth screen in the plug were 80 mesh. At each flow rate steady state fully developed velocities were measured well downstream across the diameter of the tube to check the laser doppler flowmeter calibration and also to check the location of the tube with reference to the mill table. Then velocity profiles were measured at the closest point possible to the plug. This distance, 1.25 mm., was measured with the laser optics. Other velocity profiles were taken at various intervals from the plug using the mill table to determine the location.

EXPERIMENTAL RESULTS AND CONCLUSIONS

These measurements were made with water containing one part of polystyrene spheres 0.5 μ in diameter in 10,000 parts of water. Figures 3, 4 and 5 show velocity profiles downstream of the 40 and 80 mesh screens in a 1 cm. tube at three different Reynolds numbers. In these figures z is $(4L)/(DN_{Re})$, the dimensionless axial length, and U is the velocity divided by the average velocity. The open circles represent points on that half of the diameter close to lens, L_3, in Figure 2. The other points were measured on the other half of the diameter. The curves represent average values so that the flow rate calculated from the velocity profile fit the measured flow when there are no data near the wall of the tube or when the data scatters at very small values of z. Near the center of the tube where the velocity differences were small in the scattering volume, the arithmetic average of the velocity was used to establish the flat portion of the profile for small z. Just beyond the last screen the profile was highly irregular but for $z > 0.03$ smooth profiles were measured.

The accuracy-uncertainty of the measured velocities is estimated as $\pm 1\%$. This limit is based on the accuracy of reading the spectrum analyzer. Spot checks on measurements showed no change within this accuracy with respect to the prominent velocity peak. Measurements closest to the tube wall showed variations in the spread of velocities in the scattering volume.

A summary of flow development at the center line is shown in Figure 6. Curve 1 is a plot of the standard boundary layer solution for entrance flow starting with a flat profile. At a $N_{Re} = 460$, Curve 2 shows agreement shortly beyond the entrance. Curves 3, 4, and 5 at N_{Re} of 108, 47 and 16.5 show increasing deviations from the boundary layer analysis with decreasing Reynolds number as if the entrance starting point were displaced a small amount.

In Figure 7 center line velocities are shown as a func-

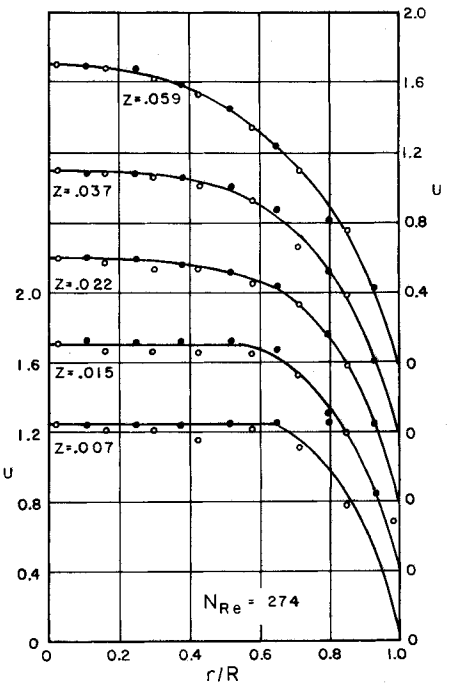

Fig. 5. Flow development in 1 cm. tube at $N_{Re} = 274$.

tion of axial distance from the entrance when the entrance configuration was changed. The boundary layer solution is shown again as Curve A for comparison. Curve C represents the data at N_{Re} of 108 in a 1 cm. diam. tube with the 40 and 80 mesh screens. By using the same plug configuration with 40 and 80 mesh screens but in a tube of ½ in. diam., Curve B was obtained at a Reynolds number of 106. The results are essentially identical for $z > 0.2$ but show significant differences closer to the plug, which is probably due to the differences in the area occupied by the screens relative to the large change in overall cross section. The final curve, D, shows the flow development when 40 mesh screens were used alone in a 1 cm. tube at a N_{Re} of 95. Data at other flow rates show the same effect, and Figure 7 is given as an example.

These curves show only the entrance region quite close to the plug, but other measurements were made at greater axial distances. These other points were used to construct the curves shown when only two or three data points are on the figures. The large difference in flow development when the 40 mesh screen sets the flow pattern, compared to the 80 mesh screen, must be due to the difference in the velocity profile at the immediate inlet. The 80 mesh screen gives smaller variations from a flat profile than the 40 mesh screen which has larger wires and larger spacings between wires.

This results in a larger amplitude disturbance at $z = 0$ for the 40 mesh screen entrance. The flow development at larger values of z was found to be 99% of its fully developed value at approximately three times the value of z for the boundary layer solution for a Reynolds number of 16.5. At higher Reynolds numbers the entrance length was smaller.

DISCUSSION

The equations of motion for entrance flow have been solved for many simplified cases by many investigators as discussed by Christiansen and Lemmon (*12*), Atkinson, et al. (*11*), Sparow, et al. (*13*), and Dealy (*14*). Tanner and Manton (*15*), Wang and Longwell (*16*), and Vrentas, et al. (*17*), have attempted to be more rigorous in their treatments. All of these solutions use boundary conditions at the entrance which are difficult to fit experimentally.

Experimental measurements by Atkinson, et al. (*11*) following a distributor to create a flat profile were found to fit boundary layer calculations at Reynolds numbers greater than 450, but no measurements were made closer than 16.5 mm. from the entrance. Goldstein and Kreid (*8*) used Reynolds numbers between 69 and 387 and found the flow to develop slower than predicted for a square duct.

The results of this work tend to confirm the conclusions

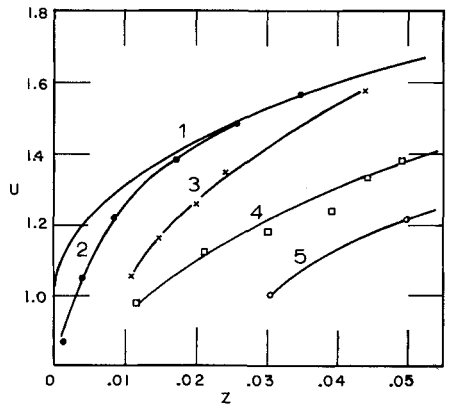

Fig. 6. Center line flow development at different Reynolds numbers in 1 cm. tube.

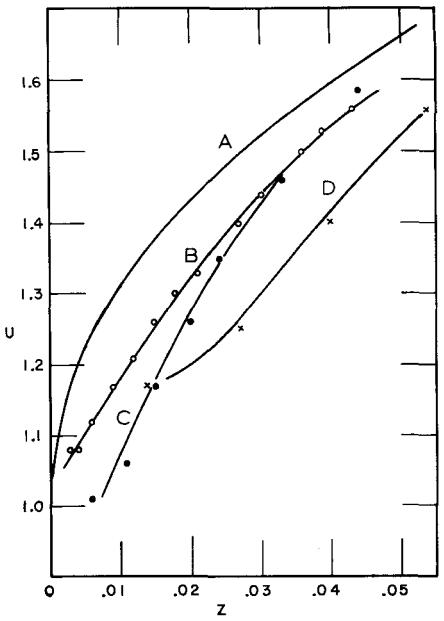

Fig. 7. Center line flow development for various entrance conditions.

of Tanner and Manton (*15*), that the flow development is not a unique quantity but depends on the inlet profile and on the Reynolds number. At Reynolds numbers of above 300 when $z > 0.02$ the boundary layer analysis using a flat entrance profile appears valid regardless of the true entrance. At lower Reynolds numbers and for $z < 0.02$ both the entrance profile and the Reynolds number are important variables. The entrance plug used in this work produces a complex entrance difficult to evaluate theoretically. Velocity gradients were present in the center of the tube as well as at the edge in this entrance profile. The results show that a complete analysis of the flow equations is necesary to properly explain entrance flow and that the laser doppler technique can be a powerful experimental tool.

ACKNOWLEDGMENT

The authors are grateful to the donors of the Petroleum Research Fund administered by the American Chemical Society and the University Grants Committee of Arizona State University who supported this work.

NOTATION

A_R = aperture area
C = velocity of light
d = aperture diameter
D = tube diameter
$\mathbf{k}_i$ = unit direction vector of incident wave
$\mathbf{k}_s$ = unit direction vector of scattered wave
L = distance downstream of plug
n = index of refraction
N_{Re} = Reynolds number
r = radial distance from center of tube
radius of tube
$\mathbf{v}$ = velocity
V = dimensionless velocity, velocity divided by average velocity
z = $4L/DN_{Re}$, dimensionless axial distance

Greek Letters

$\Delta\theta$ = angle between beams at photocell
$\Delta\nu$ = $\nu_s - \nu_i$, frequency shift
λ = wave length
λ_i = incident wave length
λ_s = scattered wave length

λ_o = vacuum wave length of light
ν_p = frequency observed by particle
ν_i = incident frequency
ν_s = scattered frequency
Ω_R = solid angle at aperture
θ = angle between incident and scattered wave

LITERATURE CITED

1. Yeh, Y., and H. Z. Cummins, *Appl. Phys. Letters*, **4**, 176 (1964).
2. Cummins, H. Z., N. Knable, and Y. Yeh, *Phys. Rev. Letters*, **12**, 150 (1964).
3. Foreman, J. W., Jr., E. W. George, and R. D. Lewis, *Appl. Phys. Letters*, **7**, 77 (1965).
4. ———, E. W. George, J. L. Jetton, R. D. Lewis, J. R. Thornton, and H. J. Watson, Inst. Elec. Electron Eng. J. Quantum Electron, **2**, 260 (1966).
5. Foreman, J. W. Jr., R. D. Lewis, J. R. Thornton, and H. J. Watson, Proc. Inst. Elec. Electron Eng., **54**, 424 (1966).
6. Welch, N. E. and W. J. Tomme, paper presented at Am. Inst. Aeron. Astronaut. meeting (1966).
7. James. R. N., H. S. Siefert, and W. R. Babcock, Am. Inst. Aeron. Astronaut. Paper no. 66-522 presented at Los Angeles (June 26, 1966).
8. Goldstein, R.S., and D. K. Kreid, *paper 67-APM-37 Am. Soc. Mech. Eng., Appl. Mech. Conf.*, Pasadena (June 26, 1967).
9. ———, and W. F. Hagen, *J. Phys. Fluids*, **10**, 1349 (1967).
10. Siegman, A. E., Proc. Inst. Elec. Electron. Eng., **54**, 1350 (1966).
11. Atkinson, B., K. Zdzislaw, and J. M. Smith, *AIChE J.*, **13**, 17 (1967).
12. Christiansen, E. B., and H. E. Lemmon, *ibid.*, **11**, 995 (1965).
13. Sparrow, E. M., S. H. Lin, and T. S. Lundgren, *J. Phys. Fluids*, **7**, 338 (1964).
14. Dealy, J. M., *AIChE J.*, **11**, 745 (1965).
15. Tanner, M. J., and R. I. Manton, *ibid.*, **12**, 816 (1966).
16. Wang, Y. L., and P. A. Longwell, *ibid.*, **10**, 323 (1964).
17. Vrentas, J. S., J. L. Duda, and K. G. Bargeron, *ibid.*, **12**, 837 (1966).

Manuscript received February 1, 1968; revision received April 1, 1968; paper accepted April 4, 1968. Paper presented at AIChE New York City meeting.

The Laminar Boundary Layer on a Moving Continuous Flat Sheet Immersed in a Non-Newtonian Fluid

V. G. FOX, L. E. ERICKSON, and L. T. FAN

Kansas State University, Manhattan, Kansas

The laminar boundary layers on a moving continuous flat surface in non-Newtonian fluids characterized by the power law model are investigated using exact and approximate methods. Both pseudoplastic and dilatant fluids are considered. Numerical solutions of the boundary-layer equations are obtained for values of the parameter n in the power law model ranging from 0.1 to 2.0. An integral solution of the momentum equation, which can be used to obtain values of the dimensionless shearing stress that are in good agreement with the exact values, is developed. An integral solution to the energy equation is also presented.

Non-Newtonian fluids are becoming increasingly important industrially. This increasing importance supplies the motivation for solving the boundary-layer equations for non-Newtonian fluids. In this paper the laminar boundary layer on a moving continuous flat surface is investigated for the case of a purely viscous fluid and zero transverse velocity at the surface. The boundary layer momentum equation is solved by an exact method and also by an integral method. Solutions for the boundary layer energy equation are obtained by an integral method. The boundary layer on a moving continuous surface in a Newtonian fluid was previously investigated (*9, 11*). However, to the best of the authors' knowledge, no such investigation has been carried out for a non-Newtonian fluid.

The non-Newtonian fluid model used in this study is the power law model (Ostwald-de Waele fluid) with the parameters defined by

$$\tau = -\left\{K\left|\sqrt{\frac{1}{2}(\Delta:\Delta)}\right|^{n-1}\right\}\Delta \qquad (1)$$

Both pseudoplastic and dilatant fluids are considered and solutions of the boundary-layer equations are obtained for values of the parameter, n, from 0.1 to 2.

The power law model, Equation (1), has been shown to be valid for a large class of non-Newtonian fluids (*1, 3*). In order to develop the expression for τ_{yx},

$$\tau_{yx} = -K\left|\frac{\partial u}{\partial y}\right|^{n-1}\frac{\partial u}{\partial y} \qquad (2)$$

from Equation (1) it is necessary to assume that $\partial u/\partial y$ is much larger than all other velocity gradients. This is the

V. G. Fox is at the University of Denver, Denver, Colorado.